Neurobiology of Disease

The Ca^{2+}-Activated K^+ Channel *KCNN4*/KCa3.1 Contributes to Microglia Activation and Nitric Oxide-Dependent Neurodegeneration

Vikas Kaushal,[1,2] Paulo D. Koeberle,[1] Yimin Wang,[1] and Lyanne C. Schlichter[1,2]

[1]Toronto Western Research Institute, University Health Network, Toronto, Ontario, Canada M5T 2S8, and [2]Department of Physiology, University of Toronto, Toronto, Ontario, Canada M5S 1A1

Brain damage and disease involve activation of microglia and production of potentially neurotoxic molecules, but there are no treatments that effectively target their harmful properties. We present evidence that the small-conductance Ca^{2+}/calmodulin-activated K^+ channel *KCNN4*/ KCa3.1/SK4/IK1 is highly expressed in rat microglia and is a potential therapeutic target for acute brain damage. Using a Transwell cell-culture system that allows separate treatment of the microglia or neurons, we show that activated microglia killed neurons, and this was markedly reduced by treating only the microglia with a selective inhibitor of KCa3.1 channels, triarylmethane-34 (TRAM-34). To assess the role of KCa3.1 channels in microglia activation and key signaling pathways involved, we exploited several fluorescence plate-reader-based assays. KCa3.1 channels contributed to microglia activation, inducible nitric oxide synthase upregulation, production of nitric oxide and peroxynitrite, and to consequent neurotoxicity, protein tyrosine nitration, and caspase 3 activation in the target neurons. Microglia activation involved the signaling pathways p38 mitogen-activated protein kinase (MAPK) and nuclear factor κB (NF-κB), which are important for upregulation of numerous proinflammatory molecules, and the KCa3.1 channels were functionally linked to activation of p38 MAPK but not NF-κB. These *in vitro* findings translated into *in vivo* neuroprotection, because we found that degeneration of retinal ganglion cells after optic nerve transection was reduced by intraocular injection of TRAM-34. This study provides evidence that KCa3.1 channels constitute a therapeutic target in the CNS and that inhibiting this K^+ channel might benefit acute and chronic neurodegenerative disorders that are caused by or exacerbated by inflammation.

Key words: **microglia activation; neurodegeneration; neuroinflammation; Ca^{2+}-activated K^+ channel; *KCNN4*/KCa3.1/IK1/SK4; optic nerve; retinal ganglion cell**

Introduction

Under pathological conditions, microglia (resident CNS immune cells) activate and can produce reactive oxygen and nitrogen species and proinflammatory cytokines: molecules that can contribute to axon demyelination and neuron death. Because some microglia functions can exacerbate CNS disorders, including stroke, traumatic brain injury, multiple sclerosis, and several retinal diseases (for review, see Minagar et al., 2002; Nelson et al., 2002; Pocock et al., 2002), controlling their activation might ameliorate immune-mediated CNS disorders. We present evidence that the Ca^{2+}-dependent K^+ channel KCa3.1 (*KCNN4*/IK1/SK4) is a potential therapeutic target for inflammation-mediated neurotoxicity in the CNS. KCa3.1 channels are well suited for roles in immune cells, requiring only a small elevation in Ca^{2+} (K_d of ~300 nM), then remaining active at physiologically relevant voltages (Mahaut-Smith and Schlichter, 1989; Ishii et al., 1997; Joiner et al., 1997; Khanna et al., 1999). KCa3.1/*KCNN4* current and expression in human T cells increase with activation and regulates proliferation of specific T cell subsets (Mahaut-Smith and Schlichter, 1989; Grissmer et al., 1993; Logsdon et al., 1997; Khanna et al., 1999; Ghanshani et al., 2000; Wulff et al., 2003); thus, it is considered a therapeutic target for disorders mediated by T lymphocytes (e.g., transplant rejection and multiple sclerosis). This channel may also directly affect CNS inflammation, because KCa3.1 currents have been observed in murine and rat microglia (Eder et al., 1997; Khanna et al., 2001), and nonselective KCa3.1 blockers implicate them in production of superoxide free radicals, a potentially neurotoxic outcome of microglia activation (Khanna et al., 2001) (for review, see Schlichter and Khanna, 2002). Here, we used lipopolysaccharide (LPS) and the KCa3.1-selective blocker triarylmethane-34 (TRAM-34) (Wulff et al., 2000) to assess whether KCa3.1 channels contribute to microglia activation and neurotoxic properties and then to elucidate the mechanisms involved.

LPS is well known to upregulate inducible nitric oxide synthase (iNOS) and increases nitric oxide (NO) production in microglia (Possel et al., 2000; Fordyce et al., 2005). The resulting neurotoxicity has been attributed to production of NO (Golde et

Received Aug. 18, 2006; revised Nov. 29, 2006; accepted Nov. 30, 2006.

L.C.S. was supported by Canadian Institutes for Health Research Grant MT-13657 and Heart and Stroke Foundation, Ontario Chapter, Grants T4670 and T5546. P.D.K. was supported by a fellowship from the Heart and Stroke Foundation. We thank Xiaoping Zhu and Chris Fordyce for technical assistance.

Correspondence should be addressed to Lyanne C. Schlichter, Toronto Western Hospital, MC9-417, 399 Bathurst Street, Toronto, Ontario, Canada M5T 2S8. E-mail: schlicht@uhnres.utoronto.ca.

DOI:10.1523/JNEUROSCI.3593-06.2007

 0270-6474/07/270234-11$15.00/0

al., 2003), which inhibits mitochondrial respiration, and to peroxynitrite, a highly reactive molecule that nitrates tyrosine residues on membranes and triggers apoptosis of target cells (for review, see Bolanos et al., 1997). There is no information linking KCa3.1 channels to these processes; therefore, we used TRAM-34 to examine iNOS induction and NO production and processes underlying their ability to kill healthy neurons. Next, to determine whether KCa3.1 channels are involved in signaling pathways by which LPS activates microglia, we examined the mitogen-activated protein kinase (p38 MAPK) and the transcription factor nuclear-factor-κB (NF-κB). After LPS binds to the Toll-like receptor 4, these pathways are important for upregulation of numerous inflammatory molecules (for review, see Zielasek and Hartung, 1996). Finally, we addressed whether KCa3.1 channels are likely to be a good therapeutic target for rescuing CNS neurons from inflammation-mediated degeneration *in vivo*. Because we found robust *KCNN4* mRNA expression in both the healthy and damaged retina, we used intraocular TRAM-34 injections to examine the role of KCa3.1 channels in the apoptotic death of retinal ganglion cells (RGCs) after optic nerve transection.

Parts of this work have been published previously in abstract form (Schlichter et al., 2005).

Materials and Methods

Cell cultures and treatments. Animal handling followed guidelines from the Canadian Council on Animal Care. Microglia were purified from whole brains of 1- to 2-d-old Wistar rat pups (Charles River, St. Constant, Quebec, Canada) as described previously (Khanna et al., 2001; Fordyce et al., 2005). Briefly, after 10–12 d of culturing, microglia were harvested by shaking the flasks on an orbital shaker (80 rpm, 4–6 h, 37°C) and seeded in serum-free Neurobasal A medium with 2% B27 supplement, 0.05 mg/ml gentamycin, and 0.5 mM L-glutamine (all from Invitrogen, Carlsbad, CA). Astrocyte purity was increased by culturing for 2–3 d, shaking, and removing the nonadherent microglia. Neuron cultures were prepared as described previously (Fordyce et al., 2005), except that embryonic day 18 rat embryos were used, and the cultures were grown for 7–10 d to increase the proportion of mature neurons. Cells were seeded on poly-L-ornithine (Sigma, St. Louis, MO)-treated German coverslips (Bellco Glass, Vineland, NJ) at 3×10^4 cells per well in the medium described above.

When desired, microglia were activated with 100 ng/ml LPS (Sigma), which is commonly used to activate these cells (for review, see Zielasek and Hartung, 1996) without cytotoxicity (Xie et al., 2002; present study). The selective KCa3.1 channel blocker TRAM-34 (gift from Dr. H. Wulff, University of California, Davis, Davis, CA; or synthesized by Toronto Research Chemicals, North York, Toronto, Canada) was dissolved in DMSO and used at 1 μM. As expected from its K_d of 20–25 nM (Wulff et al., 2000; Chandy et al., 2004), we found that this concentration blocked >95% of the KCa3.1 current in transfected CHO cells (data not shown). Even much higher concentrations do not affect other microglial channels, including SK1–SK3, Kv1.3, or Kir2.1 (Wulff et al., 2000). All statistical comparisons were made between TRAM-34 and the solvent (DMSO) control, and we also confirmed that DMSO had no effect. When exposing neuron cultures to microglia, experiments were divided into two phases, as follows. (1) Microglia (10^6 cells per well) were grown on porous upper inserts of Transwell chambers (BD Biosciences, Franklin Lakes, NJ) in 24-well plates and incubated overnight before stimulation. After treatment with LPS for 24 h, with or without TRAM-34 or the iNOS inhibitor S-methylisothiourea (SMT) (Calbiochem, La Jolla, CA), the inserts were thoroughly washed; thus, target neuron cultures were never exposed to LPS, TRAM-34, or SMT. (2) The washed insert (with 3 μm diameter pores) bearing microglia was placed above naive cortical neurons growing on a coverslip in the bottom well of the Transwell chamber, allowing diffusion of soluble molecules. The chamber was incubated for 24 or 48 h, with or without the peroxynitrite scavenger [5,10,15,20-tetrakis (*N*-methyl-4′-pyridyl)porphinato iron (III) chloride] (FeTmPyP) (Calbiochem).

KCa3.1 immunohistochemistry. Microglia mounted on coverslips were washed with PBS (three times for 5 min each), fixed for 30 min in 4% paraformaldehyde, washed (three times for 5 min each), permeabilized for 2 min on ice with 0.01% Triton X-100, and washed again (three times for 5 min each). The cells were labeled with a rabbit polyclonal KCa3.1/SK4 antibody (1:200; Alomone Labs, Jerusalem, Israel) (18 h, 4°C) and then washed with PBS (three times for 5 min each) and labeled (2 h, room temperature) with a cyanine 3 (Cy3)-conjugated secondary antibody (1:500; Jackson ImmunoResearch, West Grove, PA). After a final wash with PBS (three times for 5 min each), the coverslips were mounted on glass slides with 1:1 glycerol/PBS for viewing.

Whole-cell patch-clamp recording. Microglia on coverslips were mounted in a perfusion chamber (model RC-25; Warner Instruments, Hamden, CT), and the tissue culture medium was replaced with an extracellular (bath) solution containing the following (in mM): 125 $NaMeSO_4$, 5 $KMeSO_4$, 1 $MgCl_2$, 1 $CaCl_2$, 5 glucose, and 10 HEPES, pH 7.4. Whole-cell currents were recorded at room temperature (22 ± 1°C) with an Axopatch-200A amplifier and pClamp version 9 software (Molecular Devices, Palo Alto, CA), and compensated on-line for series resistance and capacitance (for recording details, see Newell and Schlichter, 2005). Pipettes (3–4 MΩ resistance) were filled with a solution buffered to 1.0 μM free Ca^{2+}, which contained the following (in mM): 133 $KMeSO_4$, 2 KCl, 2 K_2ATP, 0.9 $CaCl_2$, 1 EGTA, and 10 HEPES, pH 7.2. These low-Cl^- solutions eliminated the swelling-activated Cl^- current.

Plate-reader assays. Microglia on Transwell inserts or neurons on coverslips were washed with PBS (three times for 5 min each), fixed for 30 min in 4% paraformaldehyde, washed, permeabilized for 2 min on ice with 0.01% Triton X-100, and placed in 24-well black-walled plates (PerkinElmer, Woodbridge, Ontario, Canada). Rabbit polyclonal antibodies were used to monitor total p38 MAPK (1:750; Cell Signaling Technology, Beverley, MA), phospho-p38 MAPK (1:50 for plate reader; 1:750 for Western blots; Cell Signaling Technology), inhibitory κB-α (IκB-α) (1:100; Santa Cruz Biotechnology, Santa Cruz, CA), and iNOS was monitored with a mouse monoclonal (1:200; Cell Signaling Technology). Neurons were fixed (2% glutaraldehyde and 2% paraformaldehyde) and labeled with a rabbit polyclonal nitrotyrosine antibody (1:200; Cell Signaling Technology). Primary antibody labeling (18 h, 4°C) was followed (2 h, room temperature) by the appropriate Cy3-conjugated secondary antibody (1:500; Jackson ImmunoResearch). A fluorescence plate reader (SPECTRAmax Gemini EM; Molecular Devices, Sunnyvale, CA) was used to measure the fluorescence intensity of each well. Background subtraction was done using control wells without primary antibody. Protein concentrations were measured with a Bio-Rad (Hercules, CA) colorimetric protein assay and BSA standards (Bio-Rad), using an ELISA plate reader (model EL311SX; Bio-Tek Instruments, Winooski, VT). Plate-reader-based signals were standardized as relative fluorescence units (RFU) per milligram of protein in each well. For each treatment, an average RFU per milligram of protein was obtained from three coverslips of cells cultured from one animal, and multiple *n* values were obtained using cultures from different animals. Nitric oxide production by microglia was quantified with the Griess assay according to the protocol of the manufacturer (Invitrogen), as absorbance at 450 nm from the ELISA plate reader.

Assessing neuron damage. DNA damage was determined by terminal deoxynucleotidyl transferase-mediated biotinylated UTP nick end labeling (TUNEL), according to the protocol of the manufacturer (Roche Applied Science, Laval, Quebec, Canada), and fluorescence was detected using FITC-conjugated streptavidin (1:500; Invitrogen). Control wells with no terminal transferase were included to determine background. To validate the new plate-reader method (above), results were compared with conventional cell counting, as follows. After fixation and washing, coverslips were stained for TUNEL and 4′,6′-diamidino-2-phenylindole (DAPI) (1:3000; Sigma) for 5 min, washed, and mounted on glass slides with 1:1 glycerol/PBS. Cells were imaged at room temperature with a Zeiss (Oberkochen, Germany) Axioplan 2 epifluorescence microscope and 20× quartz objective, photographed with a Zeiss digital camera (Axiocam HRm, black and white), and imaged with Zeiss Axiovision

Table 1. Primers used for real-time RT-PCR

Gene	GenBank accession number	Primers (5′-3′)
KCNN4	AJ133438	F, GCTGGAGCAGGAGAAGAGG
		R, AAAGGAGGAAGGCAGTGG
CR3	NM_012711	F, TGC TGAGACTGGAGGCAAC
		R, CTCCCCAGCATCCTTGTTT
MHC II	AJ554214	F, CCAACACCCTCATCTGCTTT
		R, AAGCCATCTTGTGGAAGGAA
GFAP	BC088851	F, CAGCTTCGAGCCAAGGAG
		R, TGTCCCTCTCCACCTCCA
Synaptophysin	NM_012664	F, GTGCCAACAAGACGGAGAGT
		R, ATCTTGGTAGTGCCCCCTTT
TBP	XM_217785	F, GCACAGGAGCCAAGAGTG
		R, GTTGGTGGGTGAGCACAAG

CR3, complement receptor 3; TBP, TATA-box binding protein; F, Forward; R, reverse.

release 4.4 software. For each cell culture (from *n* separate animals) and each experimental condition, TUNEL-positive and DAPI-positive cells were counted in five microscope fields (150–200 cells per field) on two coverslips and averaged. To further examine whether neuron death was apoptotic, caspase 3 activity was measured after neuron cultures were exposed to microglia, treated with or without LPS or TRAM-34. The cells in the lower Transwell chamber were scraped and harvested and solubilized, and the supernatant was mixed with the fluorescent synthetic substrate Ac-DEVD-AMC (*N*-acetyl-L-aspartyl-L-glutamyl-L-valyl-L-aspartic acid amide 7-amino-4-methylcoumarin) according to the protocol of the manufacturer (Calbiochem). The fluorescence intensity (excitation, 360 nm; emission, 460 nm) was determined with the plate reader and standardized to protein content, as described above.

Optic nerve transection, drug injection, and cell counting. The left optic nerve of adult female Sprague Dawley rats (225–250 g; Charles River) was transected within 1.5 mm of the eye under chloral hydrate anesthesia (Koeberle and Ball, 1999). A small piece of Gelfoam soaked in 3% Fluorogold was immediately placed on the cut optic nerve stump to retrograde label RGCs. The vitreous chamber of the eye was injected with 3 μl of TRAM-34 in DMSO, immediately after surgery and at 4 d after axotomy, the time at which RGC death is first observed. Injections were posterior to the limbus of the eye, using a pulled glass micropipette, to ensure that the anterior ocular structures were not damaged. Control intraocular injections consisted of sterile PBS with or without the vehicle, DMSO. At 14 d after optic nerve transection, rats were killed using 7% chloral hydrate anesthetic. Eyes were enucleated, the cornea and lens were removed, and the eye cup was fixed (1.5 h, room temperature) in 4% paraformaldehyde in PBS containing 2% sucrose and then washed with PBS for 15 min. The neural retina was dissected, flat mounted in 1:1 glycerol/PBS, viewed at room temperature with a Zeiss LSM 510 confocal microscope using a 20× quartz objective, and analyzed with Zeiss LSM 510 software version 3.2 SP2 software provided with the microscope. Surviving Fluorogold-labeled RGCs were counted in 70,000 μm^2 areas, and densities are expressed as number per square millimeter.

Real-time quantitative reverse transcription (qRT)-PCR was used to monitor gene transcript levels, using primers (Table 1) designed with the "Primer3Output" program (http://frodo.wi.mit.edu/cgi-bin/primer3/primer3_www.cgi). RNeasy mini kits (Qiagen, Mississauga, Ontario, Canada) were used to isolate RNA after degrading any contaminating DNA with DNaseI (0.1 U/ml, 15 min, 37°C; Amersham Biosciences, Baie d'Urfe, Quebec, Canada). A two-step reaction was performed according to the instructions of the manufacturer (Invitrogen): total RNA (2 μg) was reverse transcribed using 200 U of SuperScriptII RNase H-reverse transcriptase, with 0.5 mM dNTPs (Invitrogen) and 0.5 μM oligo-dT (Sigma). Amplification was performed on an ABI PRISM 7700 Sequence Detection System (PE Biosystems, Foster City, CA) at 95°C for 10 min, followed by 40 cycles at 95°C for 15 s, 55°C for 15 s, and 72°C for 30 s. "No-template" and "no-amplification" controls (Bustin and Nolan, 2004) were included for each gene. Relative input RNA amounts were determined from a relative standard curve for each gene of interest and the housekeeping gene *TATA-box binding protein*. The efficiency of each reaction was calculated from a standard curve made by diluting the input mRNA, and data are presented as $(1 + \text{efficiency})^{-\Delta CT}$ (Pfaffl, 2001) (ABI Prism 7700 User Bulletin 2, 2001), unless otherwise indicated. Of note, correcting for the slightly different reaction efficiencies made no qualitative difference to the results.

Results

KCNN4 mRNA expression

mRNA expression for *KCNN4* (KCa3.1/SK4/IK1) was compared in neuron, astrocyte, and microglia cell cultures whose purity was assessed by immunohistochemistry and qRT-PCR (Fig. 1). Based on cell counting (Fig. 1*A*), after 7 d of culturing, the neuron cultures contained >70% MAP-2-positive cells (mature neurons), the remaining cells being astrocytes that labeled with glial fibrillary acidic protein (GFAP). Microglia cultures were >99% pure, as judged by staining with tomato lectin, which binds to cell surface *N*-acetyl-glucosamine and to *N*-acetyl-lactosamine in activated lysosome membranes (Acarin et al., 1994; Bass et al., 1998). The same results were obtained with qRT-PCR, using complement receptor 3 for microglia, synaptophysin for neurons, and GFAP for astrocytes. In Figure 1*B*, relative mRNA expression was calculated with respect to the housekeeping gene *TATA-box binding protein* (see Materials and Methods). To facilitate comparisons with cell counts, the proportional signal contributed by each cell-specific marker was calculated after setting the total signal in each cell culture to 100%. The cortical neuron cultures contained ~70% neurons and ~30% astrocytes, and both microglia and astrocyte cultures were 97–99% pure.

Next (Fig. 1*C*), the *KCNN4* mRNA expression in each cell culture was compared. Low *KCNN4* mRNA levels were present in the astrocyte and neuron cultures, with some in the neuron cultures deriving from the contaminating astrocytes. Most importantly, microglia expressed much more *KCNN4* mRNA than astrocyte or neuron cultures, and activating microglia with LPS did not change this expression. Cultured microglia labeled with an anti-KCa3.1 antibody (Fig. 1*D*), and, in accord with the lack of change in mRNA level, there was no apparent change in staining intensity after LPS. Because the microglia morphology changes profoundly after LPS treatment (processes retract, cell bodies enlarge), it is not feasible to make quantitative comparisons of staining intensity.

Blocking KCa3.1 channels in microglia reduces their neurotoxic behavior

We next asked whether inhibiting SK4 channels in microglia reduces their ability to activate and damage cultured neurons. It was necessary to rely on a KCa3.1-selective drug, TRAM-34, rather than small interfering RNA-mediated knockdown because, despite considerable testing (>15 different transfection reagents, several retroviral, and lentiviral constructs), none yielded effective transfection or infection, and most treatments were toxic to the microglia or activated them. As shown in Figure 1*E*, TRAM-34 was used to isolate the KCa3.1 current in cultured rat microglia, because it was extremely small compared with the prevalent inward-rectifier (Kir2.1) and outward rectifier (Kv1.3) currents. The TRAM-34-sensitive component was isolated by a point-by-point subtraction of the current before and after adding the drug. This KCa3.1 current was small and noisy, reversed near the K^+ Nernst potential (approximately −85 mV) was active over the entire voltage range examined, and showed the slight relaxation at very positive potentials that was described previously (Khanna et al., 1999).

To test the hypothesis that KCa3.1 channels are involved in the ability of activated microglia to kill neurons, microglia were

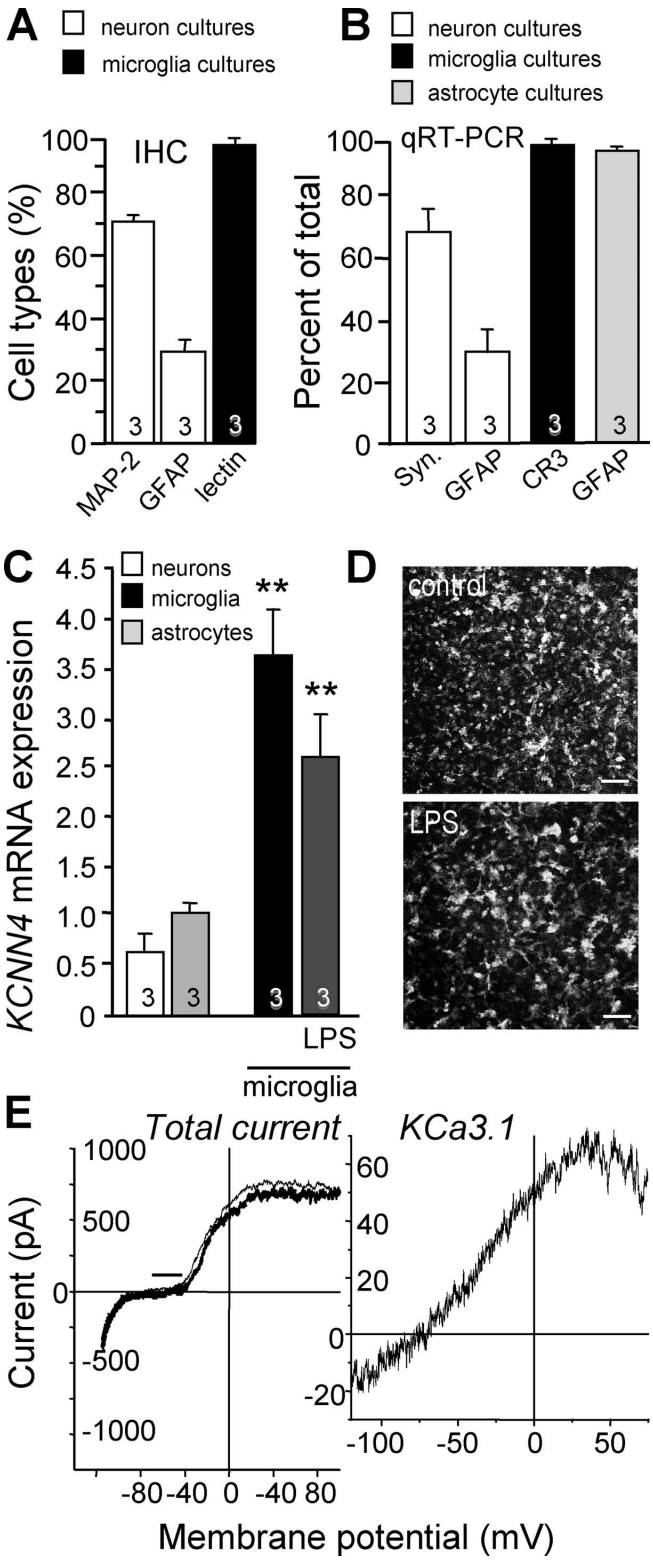

Figure 1. *KCNN4* mRNA expression in neuron, microglia, and astrocyte cultures and KCa3.1 protein and current in microglia. ***A***, The composition of the cell cultures was assessed by immunohistochemistry using a MAP-2 antibody for neurons (1:200; Sigma), an anti-GFAP antibody for astrocytes (1:200; Sigma), and FITC-conjugated tomato lectin (1 μg/ml; Sigma) for microglia. ***B***, From qRT-PCR for GFAP, synaptophysin (neurons), and complement receptor 3 (microglia), the relative mRNA levels were expressed as a percentage of the total signal (explained further in Materials and Methods and Results). ***C***, Relative *KCNN4* mRNA expression was monitored by qRT-PCR in cell cultures whose purity was assessed as in ***B***. Expression was higher in microglia than in astrocyte or neuron cultures (**$p < 0.01$) and was unchanged by treating microglia with LPS (100 ng/ml, 24 h). In this and all subsequent figures, bar graphs represent mean ± SEM for the number of separate cell cultures indicated (**$p < 0.01$). For all figures except Figure 5*E*, statistical analyses used ANOVA, followed by Bonferroni's *post hoc* tests. ***D***, KCa3.1 antibody labeling of cultured microglia. Left, Untreated microglia. Right, After 24 h treatment with LPS (100 ng/ml). Scale bars, 100 μm. ***E***, Isolation of the KCa3.1 current as the TRAM-34 blockable component of the whole-cell current. Left, Total whole-cell K^+ currents in a rat microglial cell, using a pipette solution with 1 μM free Ca^{2+} (see Materials and Methods), before (thin current trace) and after (thicker trace) adding 1 μM TRAM-34 to the bath. The black bar on the voltage axis shows the normal resting potential range recorded in primary rat microglia (Newell and Schlichter, 2005). Right, The small KCa3.1 current (i.e., TRAM-34-sensitive component) was revealed by point-by-point subtraction of the two traces in the left. Note the change in scale of the *y*-axis.

activated with 100 ng/ml LPS. Most importantly, the target neuron cultures in the lower chamber were never exposed to LPS or TRAM-34. After cell fixation, DNA damage was assessed by counting TUNEL-positive nuclei as a percentage of total DAPI-stained cell nuclei and by measuring changes in TUNEL fluorescence intensity with a plate reader. We confirmed that the TUNEL-positive cells were neurons, not contaminating astrocytes, because almost no cells colabeled with GFAP, and astrocyte cultures exposed to LPS-treated microglia did not become TUNEL-positive during the relevant 48 h time period. After 48 h incubation with unstimulated microglia, 12 ± 0.1% of the target neurons were TUNEL positive (Fig. 2*A*) compared with <1% in the absence of microglia. TUNEL-positive neurons increased to 22 ± 1% ($p < 0.01$) after exposure to LPS-activated microglia, whereas the vehicle, DMSO, had no effect. Because TUNEL expression represents a snapshot in time, some dead neurons could have detached when the wells were washed; however, the same result was seen with the caspase 3 assay (below), which did not require washing. When TRAM-34 was present during the LPS treatment, the microglia-mediated killing of target neurons was decreased ($p < 0.01$) (Fig. 2*A*) to the control level. Moreover, neither TRAM-34 nor DMSO affected microglia viability, as judged by lactate dehydrogenase release or by Alamar blue staining (data not shown). A similar result was obtained with the more efficient spectrofluorometric analysis (Fig. 2*B*), wherein mean TUNEL fluorescence intensity was measured from thousands of neurons on each coverslip and reported as RFU, standardized to the protein content for each well (see Materials and Methods). LPS-activated microglia increased TUNEL staining ($p < 0.05$), whether the vehicle was saline or DMSO, whereas, 1 μM TRAM-34 fully abrogated this excess killing ($p < 0.001$). Then, because TUNEL can represent both apoptosis and necrosis

←

(Labat-Moleur et al., 1998), caspase 3 activity was used as an additional indicator of apoptotic cell death (Gorman et al., 1998). After 24 h exposure to LPS-treated microglia (Fig. 2*C*), caspase 3 activity in the target neuron cultures increased by ~70% ($p < 0.05$), and TRAM-34 reduced this activation by ~64% ($p < 0.05$). Together, our results show that the neurotoxic activity of LPS-activated microglia was dramatically reduced by blocking their KCa3.1 channels.

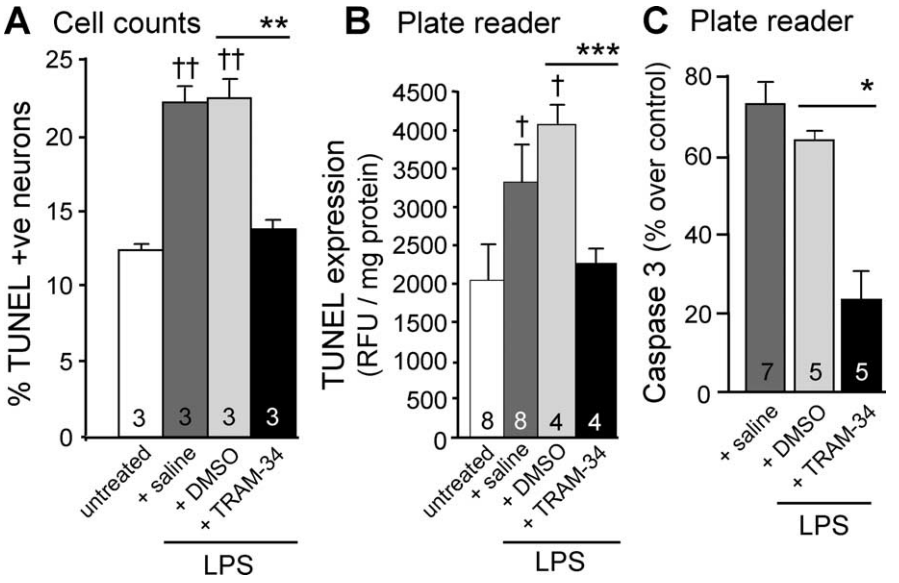

Figure 2. Blocking KCa3.1 channels in microglia reduces their neurotoxic behavior. Microglia on Transwell inserts were incubated with LPS (100 ng/ml, 24 h), with or without 1 μM TRAM-34 or the vehicle (DMSO), and then washed to remove the drugs; thus, the target neurons were not exposed to LPS or TRAM-34. Each insert was then placed in a Transwell chamber above healthy neurons and incubated for 24 h (for caspase 3 activation) or 48 h (for TUNEL), and then the target neuron cultures were removed and assayed. Data are presented as mean ± SEM. ***A***, TUNEL-positive nuclei were counted and expressed as a percentage of all DAPI-stained nuclei. TUNEL-positive cells were neurons (see Results). LPS-stimulated microglia killed more neurons than untreated microglia ($^{\dagger\dagger}p < 0.01$), and this was prevented by TRAM-34 treatment ($^{**}p < 0.01$). ***B***, Average TUNEL fluorescence was monitored with a plate reader, as RFU per milligram of protein measured in each neuron-containing well. Again, LPS-stimulated microglia killed more neurons ($^{\dagger}p < 0.05$), and this was prevented by TRAM-34 ($^{***}p < 0.001$). ***C***, The average caspase-3 activity in wells containing target neuron cultures was monitored using a fluorogenic substrate (Ac-DEVD-AMC) and the fluorescence plate reader. Results were normalized to the signal resulting from exposure to untreated microglia. TRAM-34 reduced caspase-3 activation ($^{*}p < 0.05$).

Mechanism of neuroprotection by KCa3.1 channel blockade

Microglia activation is often accompanied by increased iNOS and NO production (Dheen et al., 2005). Neurotoxicity by NO can be direct, by inhibiting mitochondrial respiration (Baud et al., 2004), or indirect, when peroxynitrite oxidizes cellular proteins, lipids, and nucleic acids (Zhu et al., 2004). Based on the known role of peroxynitrite in neuron killing by microglia (Xie et al., 2002; Fordyce et al., 2005), we used the same experimental approach as above to assess whether iNOS and peroxynitrite contribute to the neurotoxicity. The increased TUNEL signal in the target neurons (Fig. 3*A*) was substantially reduced by adding the iNOS inhibitor SMT (Calbiochem) at the same time as the LPS ($p < 0.05$) or by adding the peroxynitrite scavenger FeTmPyP (Calbiochem) during the incubation of microglia with target neurons ($p < 0.05$).

Although KCa3.1 channels are present in microglia (Eder et al., 1997; Khanna et al., 2001; Schlichter and Khanna, 2002), nothing is known about their involvement in iNOS induction and NO production. We found that LPS stimulation (100 ng/ml, 24 h) greatly increased iNOS protein levels in microglia (measured by spectrofluorometry; $p < 0.05$) (Fig. 3*B*), and this induction was strongly inhibited by blocking KCa3.1 channels (1 μM TRAM-34 vs DMSO control; $p < 0.05$). Although lower iNOS levels should result in less NO production, it is important to directly monitor NO, because iNOS activity might also be affected. LPS stimulation increased NO production more than threefold ($p < 0.025$) (Fig. 3*C*), and this was completely abrogated by TRAM-34 ($p < 0.01$). Finally, because high NO levels and peroxynitrite can affect neuron viability through protein nitration (Alvarez and Radi, 2003), we monitored tyrosine nitration levels of proteins in the target neuron cultures. As shown in Figure 3*Di*, there was some nitrotyrosine staining in control neuron cultures exposed to unstimulated microglia (conditions under which ~12% of neurons died), and neuronal staining increased after exposure to LPS-treated microglia. These changes, quantified with the fluorescence plate reader, showed that exposure to LPS-treated microglia increased neuronal tyrosine nitration by ~1.6-fold ($p < 0.05$) (Fig. 3*Dii*), whereas, nitration was reduced to below control levels when the microglia were pretreated with TRAM-34 ($p < 0.01$). This result is consistent with the effects of TRAM-34 on iNOS and NO production by microglia.

Blocking KCa3.1 channels inhibits activation of p38 MAPK, but not NF-κB, in microglia

Signal transduction pathways involving p38 MAPK and NF-κB contribute to microglia activation and production of proinflammatory molecules (Pawate et al., 2004) that can lead to neurotoxicity *in vivo* (for review, see Zhang and Stanimirovic, 2002). Therefore, we examined whether activation of either pathway is affected by KCa3.1 channel blockade. p38 MAPK activation was measured using a standard technique, wherein its phosphorylated active form is monitored with a phospho-p38-specific antibody. The plate-reader assay was validated by comparison with Western blotting, which we described previously (Fordyce et al., 2005). Spectrofluorometric monitoring of phospho-p38 MAPK (Fig. 4) showed that treating microglia with 100 ng/ml LPS transiently activated p38 MAPK (Fig. 4*Ai*), and, based on the robust increase at ~30 min, this time was chosen for all additional experiments. A representative Western blot (Fig. 4*Aii*) confirmed the increase in phospho-p38 protein, with no change in total p38 MAPK. Our finding that TRAM-34 reduced phospho-p38 by ~73% compared with the DMSO control after LPS stimulation ($p < 0.05$) (Fig. 4*B*) provides the first evidence that KCa3.1 channels are involved in p38 MAPK phosphorylation/activation in any cell type. We next examined NF-κB signaling, which begins with phosphorylation and degradation of IκB-α, a key component of the cytoplasmic NF-κB complex (Viatour et al., 2005). This releases the p50 and p65 subunits that translocate to the nucleus and promote transcription of proinflammatory genes (Chan and Murphy, 2003). In Figure 4*C*, a standard approach was used to assess NF-κB activation, which monitors degradation of IκB-α (Nikodemova et al., 2006). As expected, LPS treatment

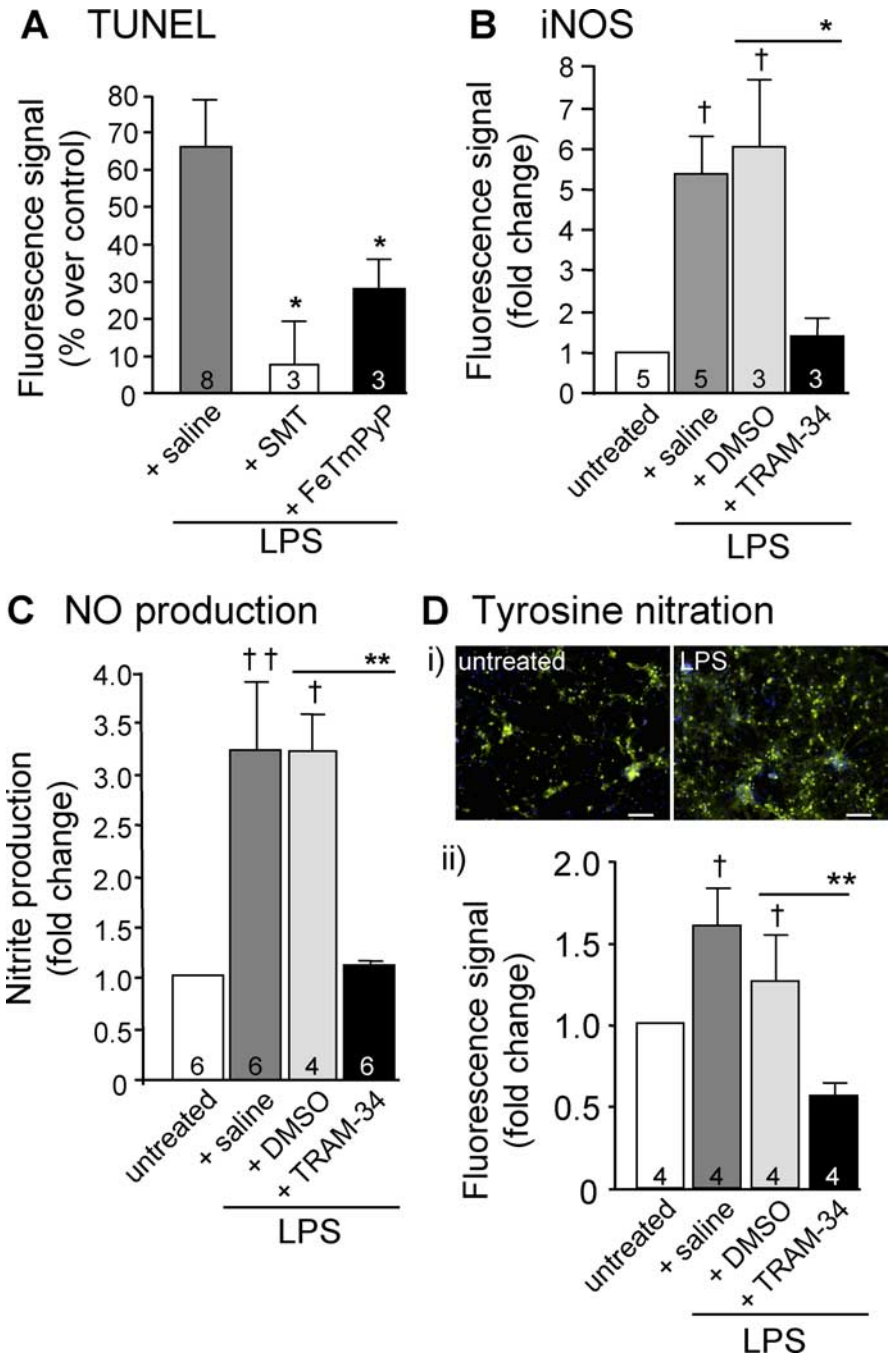

Figure 3. Mechanism of neuroprotection by KCa3.1 channel blockade. ***A***, Microglia were grown on Transwell inserts and treated with LPS, and the TUNEL intensity was measured as in Figure 2. When used, the iNOS inhibitor SMT (100 μM) was added to the microglia cultures, and, after washing, the inserts were placed above healthy neurons for 48 h. When used, the peroxynitrite scavenger FeTmPyP (2 μM) was added for 48 h to the final Transwell chambers containing microglia and neuron cultures. Both compounds reduced neuron killing ($^{*}p < 0.05$). ***B***, iNOS protein was measured in microglia using the fluorescence plate reader and an anti-iNOS antibody, with or without 1 μM TRAM-34. Readings were normalized to the fluorescence intensity in untreated microglia. LPS stimulation increased microglial iNOS ($^{\dagger}p < 0.05$), and this was prevented by 1 μM TRAM-34 ($^{*}p < 0.05$). ***C***, Nitric oxide (i.e., nitrite) production by microglia was monitored with the Griess assay and normalized to the amount produced by untreated microglia. LPS treatment increased microglial NO production ($^{\dagger\dagger}p < 0.025$), and this was prevented by 1 μM TRAM-34 ($^{**}p < 0.01$). ***D***, Same experimental design as Figure 2*B*, except that tyrosine nitration was measured in neuron cultures with an anti-nitrotyrosine antibody. ***i***, Immunostaining of neuron cultures exposed for 48 h to microglia shows nitrotyrosine labeling (green) and nuclear staining with DAPI (blue). Scale bar, 50 μm. ***ii***, Tyrosine nitration was measured with the fluorescence plate reader and normalized to the fluorescence intensity in untreated microglia. LPS-treated microglia increased tyrosine nitration in neurons ($^{\dagger}p < 0.05$), and this was prevented by treating only the microglia with 1 μM TRAM-34 ($^{**}p < 0.01$). Here and in Figure 4, untreated controls were normalized to 1.0, but statistical analyses were performed on the raw data. Data presented as mean ± SEM.

activated NF-κB in microglia, which is seen as a ~57% reduction in IκB-α levels compared with untreated microglia ($p < 0.05$). Of note, TRAM-34 did not affect this NF-κB activation; thus, KCa3.1 blockade discriminated between these two important signaling pathways. Of course, it is possible that KCa3.1 blockade also affects other microglia functions or signaling molecules that were not examined in this study.

KCa3.1 blockade *in vivo* reduces death of retinal ganglion cells after optic nerve transection

To determine whether these *in vitro* results translate to neuroprotection in the CNS *in vivo*, we used an optic nerve transection model. Microglia activate and migrate after retinal damage (Thanos and Richter, 1993) (for review, see Vilhardt, 2005), and inflammation has been implicated in the apoptotic degeneration of RGCs, which reaches 80–90% by 2 weeks after axotomy (Koeberle and Ball, 1999; Bahr, 2000; Chen et al., 2002; Koeberle et al., 2004). First (Fig. 5*A*), we conducted real-time qRT-PCR in whole retinas at 7 d after axotomy, when the rate of RGC apoptosis is maximal (for review, see Bahr, 2000; Chen et al., 2002). *KCNN4* mRNA was expressed and unaltered after axotomy, whereas major histocompatibility complex (MHC) class II, a molecule that increases when antigen-presenting cells (including microglia) are activated, was greatly upregulated (approximately eightfold; $p < 0.01$). Figure 5*B* shows key changes in the location (*Bi*) and morphology of retinal microglia after axotomy. In the healthy retina, only a few OX-42-labeled cells were present in the nerve fiber layer (NFL) (Fig. 5*Bii*), in which they had oval cell bodies and short processes, characteristic of perivascular retinal microglia (Chen et al., 2002). In the adjacent inner plexiform layer (IPL) of the healthy retina (Fig. 5*Biii*), microglia were densely packed and extensively ramified. By 14 d after axotomy (Fig. 5*Biv*), large numbers of microglia had migrated to the NFL, in which they aligned with the fascicles of degenerating RGC axons. Thus, our four lines of evidence for microglia activation after axotomy are migration, realignment along the axons, a less ramified morphology, and upregulation of MHC class II mRNA.

To assess the role of KCa3.1 channels in degeneration of RGCs, intraocular injections of saline, TRAM-34, or the DMSO solvent were given at the time of axotomy and again at day 4, the time at which RGC apoptosis begins (Villegas-Perez et al.,

1988). Intraocular injection was favored over intravenous or intraperitoneal routes for two main reasons: (1) to restrict the site of drug action, avoiding effects on the peripheral immune system and other tissues that express KCa3.1 (e.g., epithelia); and (2) to ensure entry into retinal tissue and control of the initial (maximal) drug concentration within the orbit. A range of TRAM-34 concentrations was tested because diffusion out of the retina into the brain parenchyma is likely to be slow and incomplete (Ghate and Edelhauser, 2006). Care was taken to avoid puncturing the lens, which evokes release of soluble growth factors (Leon et al., 2000). At 1 d after axotomy (Fig. 5*Ci*), large numbers of Fluorogold-labeled RGCs were seen, along with more faintly labeled axon bundles. In contrast, by 14 d after axotomy, most of the RGCs had degenerated (Fig. 5*Bii*), and many microglia contained neuronal debris (Fig. 5*Cv*). Intraocular TRAM-34 injections increased the numbers of surviving RGCs (Fig. 5*Ciii*,*Civ*) but did not affect the microglia relocation, realignment, or morphological changes seen after axotomy (Fig. 5, compare *Cvi* with *Biv*). To compare RGC densities at 14 d after axotomy (Fig. 5*D*), Fluorogold-labeled RGC cell bodies were counted in flat-mounted retinas, from four fields for each retinal region (inner, midperiphery, and outer). TRAM-34 (5 or 50 μM) produced a 2- to 2.5-fold increase in RGC density compared with either saline- or DMSO-injected controls ($p < 0.05$). Together, our results provide evidence that blocking KCa3.1 channels reduces microglia activation and neuron killing *in vitro* and that a decrease in production of neurotoxic factors renders TRAM-34 neuroprotective after traumatic CNS injury *in vivo*.

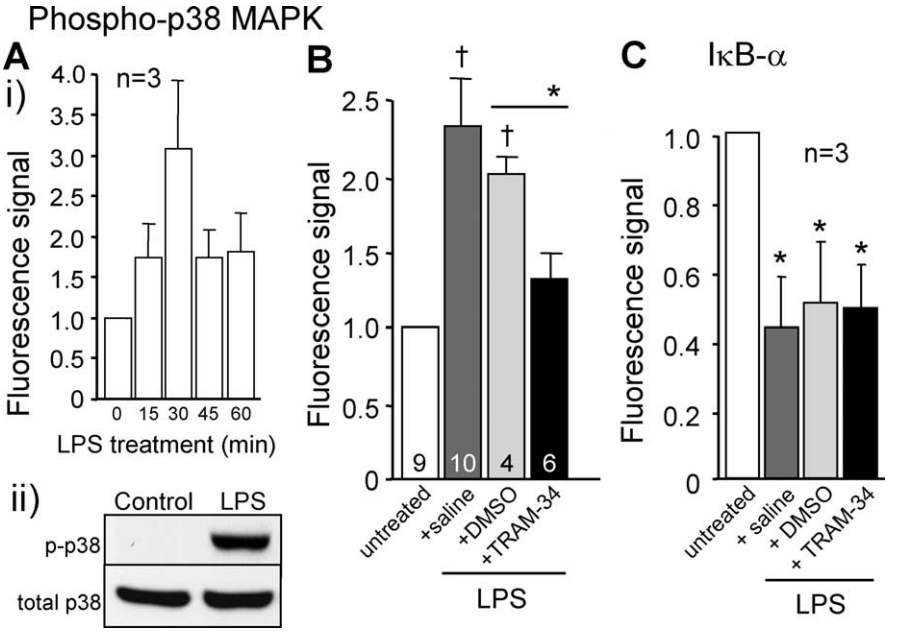

Figure 4. Blocking KCa3.1 channels inhibits activation of p38 MAPK but not NF-κB, in microglia. Microglia cultures were treated with LPS (100 ng/ml), with or without 1 μM TRAM-34. p38 MAPK activation was monitored with an antibody that recognizes phosphorylated (active) phospho-p38 MAPK, after which the gel was stripped and reprobed with a p38 MAPK antibody. NF-κB activation was monitored as degradation of Iκ-Bα (see Results), using an Iκ-Bα antibody. The fluorescence plate reader was used (except ***Aii***), and results are normalized to the signal from untreated microglia. Data presented as mean ± SEM. ***Ai***, A time course for phospho-p38 MAPK was used to establish an optimal time for examining subsequent drug effects. ***Aii***, A representative Western blot from microglia after 30 min LPS treatment. ***B***, The phospho-p38 MAPK fluorescence signal was increased in microglia after 30 min LPS treatment ($^{\dagger}p < 0.05$), and this was prevented by 1 μM TRAM-34 ($^{*}p < 0.05$). ***C***, The Iκ-Bα fluorescence signal decreased in microglia after 30 min LPS treatment ($^{*}p < 0.05$), and this was unaffected by 1 μM TRAM-34.

Discussion

Significance of findings

Among the *KCNN* family of Ca^{2+}-activated K^+ channels, *KCNN4*/KCa3.1 is thought to be restricted to non-excitable cells (Cahalan et al., 2001; Jensen et al., 2002; Schlichter and Khanna, 2002; Chandy et al., 2004). There are several key findings in the present study. Using real-time qRT-PCR, we show that (1) the *KCNN4* mRNA level in microglia does not change when they are activated *in vitro* (by LPS); (2) *KCNN4* mRNA is present in the healthy CNS (the retina); (3) the *KCNN4* mRNA level in the retina does not change 7 d after optic nerve transection, the time at which the inflammatory response is maximal; and (4) astrocytes express *KCNN4* mRNA but at a much lower level than microglia. Next, by monitoring several cellular functions, we provide the first evidence that microglial KCa3.1 channels (5) contribute to iNOS induction and nitric oxide production and (6) are functionally linked to a key signaling molecule, p38 MAPK, in a gene transcription pathway that upregulates numerous proinflammatory molecules. Then, by examining the outcome of exposing naive neurons to activated microglia, we show that microglia KCa3.1 channels contribute to (7) their neurotoxic capacity and (8) to the consequent increases in tyrosine nitration of proteins and caspase 3 activity in the target neurons. Finally, we show that (9) intraocular injection of the KCa3.1 blocker significantly reduces the degeneration of retinal ganglion cells *in vivo*. This work also demonstrates the utility of fluorescence plate-reader assays for studies of microglia activation and their effects on neurons.

KCa3.1 and cell functions

Expression of *KCNN* channels (mainly mRNA) has been examined in numerous tissues, but their roles in non-excitable cells are only beginning to be elucidated. KCa3.1 is involved in microglia functions (Khanna et al., 2001; present study), lymphocyte activation (for review, see Jensen et al., 2002; Schlichter and Khanna, 2002), volume regulation in red blood cells and lymphocytes (Brugnara et al., 1996; Khanna et al., 1999), and migration of renal epithelial cells and mast cells (Schwab et al., 1999; Cruse et al., 2006). Because SK channels are not voltage gated, they are well designed to contribute to the resting potential of non-excitable cells, including immune cells (e.g., microglia). They require only a small elevation in intracellular Ca^{2+} to activate and then are open over a wide voltage range, including very negative membrane potentials (Kohler et al., 1996; Ishii et al., 1997; Joiner et al., 1997; Khanna et al., 1999). A general role for K^+ channels is to provide a pathway for K^+ efflux, which drives the membrane potential toward the K^+ Nernst potential (approximately −85 mV in mammalian cells) and thus can counteract the depolarizing effect of Ca^{2+} influx. Maintaining a large driving force for Ca^{2+} entry is thought to be the mechanism whereby KCa3.1 channels contribute to T-cell functions (Logsdon et al., 1997; Khanna et al., 1999) (for review, see Jensen et al., 2002; Chandy et al., 2004). We found that the KCa3.1 current is very small in

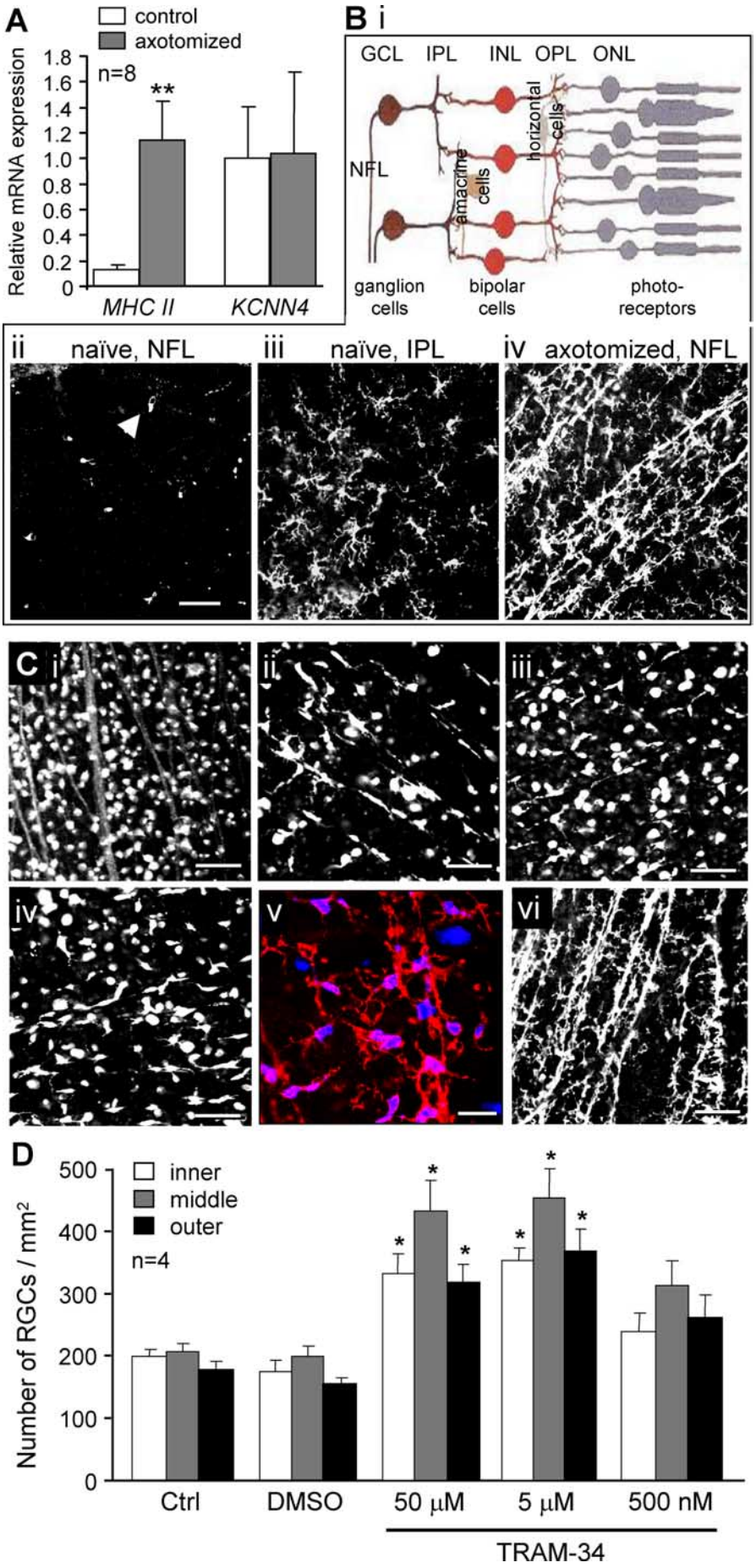

primary rat microglia and extremely difficult to separate from several other endogenous currents (especially Cl^-, inward rectifier and ERG K^+ channels, and multiple TRP channels). This small amplitude is not surprising, because we found previously that the membrane resistance of rat microglia is very high (~8 GΩ) around the resting potential (−40 to −70 mV) (Newell and Schlichter, 2005). Thus, the activity of only a few KCa3.1 channels could have a large impact on the membrane potential and microglia functions. We showed previously evidence that KCa3.1 channels contribute to the NADPH-mediated respiratory burst, which involves Ca^{2+} entry (Khanna et al., 2001; Fordyce et al., 2005) (for review, see Schlichter and Khanna, 2002). Those studies used charybdotoxin, which also blocks Kv1.3 channels, or clotrimazole, which has other cellular effects in addition to blocking KCa3.1 channels (Chandy et al., 2004). Here, we exploit the KCa3.1 blocker TRAM-34, which has excellent selectivity for KCa3.1 over other K^+ channels at the concentrations used (Wulff et al., 2000).

KCa3.1 and neurotoxicity

LPS upregulates iNOS expression and NO production in microglia (Possel et al., 2000; Fordyce et al., 2005). NO can com-

→

Figure 5. Blocking KCa3.1 channels *in vivo* reduces death of retinal ganglion cells after optic nerve transection. ***A***, mRNA expression in the healthy retina compared with 7 d after optic nerve transection (8 retinas each). mRNA levels were determined with real-time qRT-PCR and standardized as explained in Materials and Methods and Results. MHC class II expression increased after axotomy (**$p < 0.01$), whereas *KCNN4* was unchanged. ***B***, Location and morphology of OX-42-labeled retinal microglia before and after optic nerve transection. ***i***, Schematic of the retina, showing the NFL, ganglion cell layer (GCL; somata of retinal ganglion cells), the IPL, inner nuclear layer (INL), outer plexiform layer (OPL), and outer nuclear layer (ONL). ***ii–iv***, Representative confocal images. Scale bar, 50 μm. Sections from the midperiphery of flat-mounted retinas. Microglia in the NFL (***ii***) and adjacent IPL (***iii***) of the healthy retina and in the NFL (***iv***) 14 d after optic nerve transection. ***C***, Effects of intraocular TRAM-34 injection on microglia and on survival of RGCs after optic nerve transection. Scale bars, 50 μm (except as indicated). Confocal micrographs showing Fluorogold-labeled RGCs 1 d (***i***) and 14 d (***ii***) after axotomy without treatment or after intraocular injections of 5 μM (***iii***) or 50 μM (***iv***) TRAM-34 at the time of axotomy and again at day 4. ***v***, At 14 d after axotomy without treatment: OX-42-labeled microglia (red) and Fluorogold-labeled RGCs (false-colored to blue). Scale bar, 20 μm. ***vi***, OX-42-labeled microglia 14 d after axotomy, with intraocular injections of 50 μM TRAM-34. ***D***, Density of surviving RGCs 14 d after axotomy: mean ± SEM, four retinas for each condition. Statistical analyses used ANOVA, followed by Fisher's mean interval comparisons and Tukey's tests (*$p < 0.05$).

bine with superoxide, which is produced by the respiratory burst in microglia (Colton and Gilbert, 1993), to produce highly reactive peroxynitrite (Torreilles, 2001), a molecule that can exacerbate CNS damage (for review, see Bolanos et al., 1997). iNOS induction and peroxynitrite formation are thought to be the main toxic mediators when LPS-stimulated microglia are cocultured with neurons (Xie et al., 2002; Fordyce et al., 2005), and, in agreement, we found that either an iNOS inhibitor or a peroxynitrite scavenger reduced neurotoxicity. Microglia were apparently the main NO source in this model, because blocking their KCa3.1 channels with TRAM-34 prevented LPS-stimulated iNOS upregulation and NO production and was sufficient to abrogate tyrosine nitration and death of target neurons *in vitro*. These roles of KCa3.1 channels *in vitro* correspond well with the neuroprotection seen in the optic nerve transection model *in vivo*. In this model of traumatic neurodegeneration, it is known that microglia recognize and eliminate severed RGCs (Chen et al., 2002) and that iNOS inhibition reduces RGC death (Koeberle and Ball, 1999). We found that intraocular injections of TRAM-34 reduced this RGC death, providing evidence that KCa3.1 channels may be a therapeutic target for brain pathologies involving inflammation and microglia activation. Importantly, there was no evidence of drug toxicity with even the highest doses of TRAM-34, i.e., there were no seizures or changes in feeding, activity, or behavior. The outcome of microglia activation can be complex and determined primarily by the factors they produce (for review, see Zielasek and Hartung, 1996; Nelson et al., 2002; Vilhardt, 2005). Together with our *in vitro* results showing an involvement of KCa3.1 channels in microglia iNOS induction, nitric oxide production, and p38 MAPK activation, the *in vivo* results suggest that KCa3.1 blockade likely acts by reducing production and/or secretion of soluble neurotoxic molecules in the retina. Our results suggest that KCa3.1 channels are not essential for microglial shape changes, migration, or phagocytosis in the retinal damage model *in vivo*, because TRAM-34 treatment did not restore the resting microglia morphology (many remained less ramified than in the healthy retina), did not prevent their migration and realignment along axons in the ganglion cell layer, and did not prevent them from phagocytosing damaged neurons.

The proinflammatory responses of immune cells, including microglia, involve p38 MAPK and the transcription factor NF-κB (Madrid et al., 2001). There is considerable interest in using p38 MAPK inhibitors to reduce neuron death *in vivo*, for instance, after stroke (for review, see Barone et al., 2001; Zhang and Stanimirovic, 2002). LPS activates p38 MAPK and NF-κB, promoting the transcription of proinflammatory molecules, including tumor necrosis factor-α, interleukin-1β, and iNOS (Laflamme and Rivest, 1999). Although crosstalk can occur between these two pathways (Madrid et al., 2001), there is also evidence that they can mediate production of different molecules. In particular, p38 MAPK phosphorylation has been linked to iNOS induction and NO production (Barone et al., 2001; Zhang and Stanimirovic, 2002). Our studies appear to provide the first evidence that these two signaling pathways are affected by different K^+ channels. That is, blocking KCa3.1 channels in microglia inhibited p38 MAPK (but not NF-κB) activation, iNOS induction, and NO production (present study), whereas, blocking voltage-gated Kv1.3 channels inhibited NF-κB (but not p38 MAPK) activation and reduced superoxide but not nitric oxide production (Fordyce et al., 2005).

Broader implications

Potential therapeutic uses of KCa3.1 blockers were first examined for disorders involving T-cell activation, sickle cell anemia (for review, see Jensen et al., 2002; Chandy et al., 2004), and arterial restenosis (Kohler et al., 2003), and this channel is also involved in endothelial cell proliferation and angiogenesis (Grgic et al., 2005), growth of pancreatic cancer cells (Jager et al., 2004), and phenotypic modulation of coronary smooth muscle (Tharp et al., 2006). Use of KCa3.1 channel blockers to treat CNS disorders is beginning to be addressed, and the results are encouraging. Bayer (Wuppertal, Germany) developed several KCa3.1 blockers, tested them in a rat model of traumatic brain injury (subdural hematoma), and found that several hours of intravenous administration of either a triazole or a cyclohexadiene compound significantly reduced the ensuing edema, intracranial pressure, and infarct volume (Mauler et al., 2004). KCa3.1 blockade reduced inflammatory cytokine production and damage in the spinal cord in a murine model of multiple sclerosis (Reich et al., 2005), but potential contributions of CNS cells were not determined. Blocking KCa3.1 channels in endothelia and smooth muscle cells in the rat middle cerebral artery inhibited hyperpolarization and vessel relaxation (McNeish et al., 2006). Together with the roles of KCa3.1 in microglia-mediated neurodegeneration, this suggests a possible target for stroke. The present *in vitro* studies and improved survival of neurons after optic nerve transection *in vivo* provide additional evidence that blocking KCa3.1 channels can reduce microglia-induced neuroinflammation and consequent apoptotic neurodegeneration. Moreover, because microglia and peripheral macrophages share many mechanisms for proinflammatory molecule production, these results have broader implications for treating other inflammatory pathologies that involve the innate immune system.

References

Acarin L, Vela JM, Gonzalez B, Castellano B (1994) Demonstration of poly-N-acetyl lactosamine residues in ameboid and ramified microglial cells in rat brain by tomato lectin binding. J Histochem Cytochem 42:1033–1041.

Alvarez B, Radi R (2003) Peroxynitrite reactivity with amino acids and proteins. Amino Acids 25:295–311.

Bahr M (2000) Live or let die: retinal ganglion cell death and survival during development and in the lesioned adult CNS. Trends Neurosci 23:483–490.

Barone FC, Irving EA, Ray AM, Lee JC, Kassis S, Kumar S, Badger AM, Legos JJ, Erhardt JA, Ohlstein EH, Hunter AJ, Harrison DC, Philpott K, Smith BR, Adams JL, Parsons AA (2001) Inhibition of p38 mitogen-activated protein kinase provides neuroprotection in cerebral focal ischemia. Med Res Rev 21:129–145.

Bass WT, Singer GA, Liuzzi FJ (1998) Transient lectin binding by white matter tract border zone microglia in the foetal rabbit brain. Histochem J 30:657–666.

Baud O, Li J, Zhang Y, Neve RL, Volpe JJ, Rosenberg PA (2004) Nitric oxide-induced cell death in developing oligodendrocytes is associated with mitochondrial dysfunction and apoptosis-inducing factor translocation. Eur J Neurosci 20:1713–1726.

Bolanos JP, Almeida A, Stewart V, Peuchen S, Land JM, Clark JB, Heales SJ (1997) Nitric oxide-mediated mitochondrial damage in the brain: mechanisms and implications for neurodegenerative diseases. J Neurochem 68:2227–2240.

Brugnara C, Gee B, Armsby CC, Kurth S, Sakamoto M, Rifai N, Alper SL, Platt OS (1996) Therapy with oral clotrimazole induces inhibition of the Gardos channel and reduction of erythrocyte dehydration in patients with sickle cell disease. J Clin Invest 97:1227–1234.

Bustin SA, Nolan T (2004) Pitfalls of quantitative real-time reverse-transcription polymerase chain reaction. J Biomol Tech 15:155–166.

Cahalan MD, Wulff H, Chandy KG (2001) Molecular properties and physiological roles of ion channels in the immune system. J Clin Immunol 21:235–252.

Chan EL, Murphy JT (2003) Reactive oxygen species mediate endotoxin-induced human dermal endothelial NF-κB activation. J Surg Res 111:120–126.

Chandy KG, Wulff H, Beeton C, Pennington M, Gutman GA, Cahalan MD

(2004) K^+ channels as targets for specific immunomodulation. Trends Pharmacol Sci 25:280–289.

Chen L, Yang P, Kijlstra A (2002) Distribution, markers, and functions of retinal microglia. Ocul Immunol Inflamm 10:27–39.

Colton CA, Gilbert DL (1993) Microglia, an *in vivo* source of reactive oxygen species in the brain. Adv Neurol 59:321–326.

Cruse G, Duffy SM, Brightling CE, Bradding P (2006) Functional KCa3.1 K^+ channels are required for human lung mast cell migration. Thorax 61:880–885.

Dheen ST, Jun Y, Yan Z, Tay SS, Ling EA (2005) Retinoic acid inhibits expression of TNF-α and iNOS in activated rat microglia. Glia 50:21–31.

Eder C, Klee R, Heinemann U (1997) Pharmacological properties of Ca^{2+}-activated K^+ currents of ramified murine brain macrophages. Naunyn Schmiedebergs Arch Pharmacol 356:233–239.

Fordyce CB, Jagasia R, Zhu X, Schlichter LC (2005) Microglia Kv1.3 channels contribute to their ability to kill neurons. J Neurosci 25:7139–7149.

Ghanshani S, Wulff H, Miller MJ, Rohm H, Neben A, Gutman GA, Cahalan MD, Chandy KG (2000) Up-regulation of the IKCa1 potassium channel during T-cell activation. Molecular mechanism and functional consequences. J Biol Chem 275:37137–37149.

Ghate D, Edelhauser HF (2006) Ocular drug delivery. Expert Opin Drug Deliv 3:275–287.

Golde S, Coles A, Lindquist JA, Compston A (2003) Decreased iNOS synthesis mediates dexamethasone-induced protection of neurons from inflammatory injury *in vitro.* Eur J Neurosci 18:2527–2537.

Gorman AM, Orrenius S, Ceccatelli S (1998) Apoptosis in neuronal cells: role of caspases. NeuroReport 9:R49–R55.

Grgic I, Eichler I, Heinau P, Si H, Brakemeier S, Hoyer J, Kohler R (2005) Selective blockade of the intermediate-conductance Ca^{2+}-activated K^+ channel suppresses proliferation of microvascular and macrovascular endothelial cells and angiogenesis *in vivo.* Arterioscler Thromb Vasc Biol 25:704–709.

Grissmer S, Nguyen AN, Cahalan MD (1993) Calcium-activated potassium channels in resting and activated human T lymphocytes. Expression levels, calcium dependence, ion selectivity, and pharmacology. J Gen Physiol 102:601–630.

Ishii TM, Maylie J, Adelman JP (1997) Determinants of apamin and d-tubocurarine block in SK potassium channels. J Biol Chem 272:23195–23200.

Jager H, Dreker T, Buck A, Giehl K, Gress T, Grissmer S (2004) Blockage of intermediate-conductance Ca^{2+}-activated K^+ channels inhibit human pancreatic cancer cell growth *in vitro.* Mol Pharmacol 65:630–638.

Jensen BS, Hertz M, Christophersen P, Madsen LS (2002) The Ca^{2+}-activated K^+ channel of intermediate conductance: a possible target for immune suppression. Expert Opin Ther Targets 6:623–636.

Joiner WJ, Wang LY, Tang MD, Kaczmarek LK (1997) hSK4, a member of a novel subfamily of calcium-activated potassium channels. Proc Natl Acad Sci USA 94:11013–11018.

Khanna R, Chang MC, Joiner WJ, Kaczmarek LK, Schlichter LC (1999) hSK4/hIK1, a calmodulin-binding KCa channel in human T lymphocytes. Roles in proliferation and volume regulation. J Biol Chem 274:14838–14849.

Khanna R, Roy L, Zhu X, Schlichter LC (2001) K^+ channels and the microglial respiratory burst. Am J Physiol Cell Physiol 280:C796–C806.

Koeberle PD, Ball AK (1999) Nitric oxide synthase inhibition delays axonal degeneration and promotes the survival of axotomized retinal ganglion cells. Exp Neurol 158:366–381.

Koeberle PD, Gauldie J, Ball AK (2004) Effects of adenoviral-mediated gene transfer of interleukin-10, interleukin-4, and transforming growth factor-β on the survival of axotomized retinal ganglion cells. Neuroscience 125:903–920.

Kohler M, Hirschberg B, Bond CT, Kinzie JM, Marrion NV, Maylie J, Adelman JP (1996) Small-conductance, calcium-activated potassium channels from mammalian brain. Science 273:1709–1714.

Kohler R, Wulff H, Eichler I, Kneifel M, Neumann D, Knorr A, Grgic I, Kampfe D, Si H, Wibawa J, Real R, Borner K, Brakemeier S, Orzechowski HD, Reusch HP, Paul M, Chandy KG, Hoyer J (2003) Blockade of the intermediate-conductance calcium-activated potassium channel as a new therapeutic strategy for restenosis. Circulation 108:1119–1125.

Labat-Moleur F, Guillermet C, Lorimier P, Robert C, Lantuejoul S, Brambilla E, Negoescu A (1998) TUNEL apoptotic cell detection in tissue sections: critical evaluation and improvement critical evaluation and improvement. J Histochem Cytochem 46:327–334.

Laflamme N, Rivest S (1999) Effects of systemic immunogenic insults and circulating proinflammatory cytokines on the transcription of the inhibitory factor $\kappa B\alpha$ within specific cellular populations of the rat brain. J Neurochem 73:309–321.

Leon S, Yin Y, Nguyen J, Irwin N, Benowitz LI (2000) Lens injury stimulates axon regeneration in the mature rat optic nerve. J Neurosci 20:4615–4626.

Logsdon NJ, Kang J, Togo JA, Christian EP, Aiyar J (1997) A novel gene, hKCa4, encodes the calcium-activated potassium channel in human T lymphocytes. J Biol Chem 272:32723–32726.

Madrid LV, Mayo MW, Reuther JY, Baldwin AS Jr (2001) Akt stimulates the transactivation potential of the RelA/p65 Subunit of NF-κB through utilization of the IκB kinase and activation of the mitogen-activated protein kinase p38. J Biol Chem 276:18934–18940.

Mahaut-Smith MP, Schlichter LC (1989) Ca^{2+}-activated K^+ channels in human B lymphocytes and rat thymocytes. J Physiol (Lond) 415:69–83.

Mauler F, Hinz V, Horvath E, Schuhmacher J, Hofmann HA, Wirtz S, Hahn MG, Urbahns K (2004) Selective intermediate-/small-conductance calcium-activated potassium channel (KCNN4) blockers are potent and effective therapeutics in experimental brain oedema and traumatic brain injury caused by acute subdural haematoma. Eur J Neurosci 20:1761–1768.

McNeish AJ, Sandow SL, Neylon CB, Chen MX, Dora KA, Garland CJ (2006) Evidence for involvement of both IK_{Ca} and SK_{Ca} channels in hyperpolarizing responses of the rat middle cerebral artery. Stroke 37:1277–1282.

Minagar A, Shapshak P, Fujimura R, Ownby R, Heyes M, Eisdorfer C (2002) The role of macrophage/microglia and astrocytes in the pathogenesis of three neurologic disorders: HIV-associated dementia, Alzheimer disease, and multiple sclerosis. J Neurol Sci 202:13–23.

Nelson PT, Soma LA, Lavi E (2002) Microglia in diseases of the central nervous system. Ann Med 34:491–500.

Newell EW, Schlichter LC (2005) Integration of K^+ and Cl^- currents regulate steady-state and dynamic membrane potentials in cultured rat microglia. J Physiol (Lond) 567:869–890.

Nikodemova M, Duncan ID, Watters JJ (2006) Minocycline exerts inhibitory effects on multiple mitogen-activated protein kinases and I$\kappa B\alpha$ degradation in a stimulus-specific manner in microglia. J Neurochem 96:314–323.

Pawate S, Shen Q, Fan F, Bhat NR (2004) Redox regulation of glial inflammatory response to lipopolysaccharide and interferon γ. J Neurosci Res 77:540–551.

Pfaffl MW (2001) A new mathematical model for relative quantification in real-time RT-PCR. Nucleic Acids Res 29:2002–2007.

Pocock JM, Liddle AC, Hooper C, Taylor DL, Davenport CM, Morgan SC (2002) Activated microglia in Alzheimer's disease and stroke. Ernst Schering Res Found Workshop 105–132.

Possel H, Noack H, Putzke J, Wolf G, Sies H (2000) Selective upregulation of inducible nitric oxide synthase (iNOS) by lipopolysaccharide (LPS) and cytokines in microglia: *in vitro* and *in vivo* studies. Glia 32:51–59.

Reich EP, Cui L, Yang L, Pugliese-Sivo C, Golovko A, Petro M, Vassileva G, Chu I, Nomeir AA, Zhang LK, Liang X, Kozlowski JA, Narula SK, Zavodny PJ, Chou CC (2005) Blocking ion channel KCNN4 alleviates the symptoms of experimental autoimmune encephalomyelitis in mice. Eur J Immunol 35:1027–1036.

Schlichter LC, Khanna R (2002) K^+ channels and proliferation in neuroimmune cells. In: Roles of ion channels in physiopathology of nerve conduction and cell proliferation (Rouzaire-Dubois B, Benoit E, Dubois JM, eds). Trivandrum, Kerala, India: Research Signpost.

Schlichter LC, Kaushal V, Koeberle PD, Wang Y (2005) The KCNN4 (SK4/IKCA1) channel is involved in inflammation-dependent killing of CNS neurons. Soc Neurosci Abstr 31:792.13.

Schwab A, Schuricht B, Seeger P, Reinhardt J, Dartsch PC (1999) Migration of transformed renal epithelial cells is regulated by K^+ channel modulation of actin cytoskeleton and cell volume. Pflügers Arch 438:330–337.

Thanos S, Richter W (1993) The migratory potential of vitally labelled microglial cells within the retina of rats with hereditary photoreceptor dystrophy. Int J Dev Neurosci 11:671–680.

Tharp DL, Wamhoff BR, Turk JR, Bowles DK (2006) Upregulation of intermediate-conductance Ca^{2+}-activated K^+ channel (IKCa1) mediates phenotypic modulation of coronary smooth muscle. Am J Physiol Heart Circ Physiol 291:H2493–H2503.

Torreilles J (2001) Nitric oxide: one of the more conserved and widespread signaling molecules. Front Biosci 6:D1161–D1172.

Viatour P, Merville MP, Bours V, Chariot A (2005) Phosphorylation of NF-κB and IκB proteins: implications in cancer and inflammation. Trends Biochem Sci 30:43–52.

Vilhardt F (2005) Microglia: phagocyte and glia cell. Int J Biochem Cell Biol 37:17–21.

Villegas-Perez MP, Vidal-Sanz M, Bray GM, Aguayo AJ (1988) Influences of peripheral nerve grafts on the survival and regrowth of axotomized retinal ganglion cells in adult rats. J Neurosci 8:265–280.

Wulff H, Miller MJ, Hansel W, Grissmer S, Cahalan MD, Chandy KG (2000) Design of a potent and selective inhibitor of the intermediate-conductance Ca^{2+}-activated K^+ channel, IKCa1: a potential immunosuppressant. Proc Natl Acad Sci USA 97:8151–8156.

Wulff H, Calabresi PA, Allie R, Yun S, Pennington M, Beeton C, Chandy KG (2003) The voltage-gated Kv1.3 K^+ channel in effector memory T cells as new target for MS. J Clin Invest 111:1703–1713.

Xie Z, Wei M, Morgan TE, Fabrizio P, Han D, Finch CE, Longo VD (2002) Peroxynitrite mediates neurotoxicity of amyloid β-peptide$_{1-42}$- and lipopolysaccharide-activated microglia. J Neurosci 22:3484–3492.

Zhang W, Stanimirovic D (2002) Current and future therapeutic strategies to target inflammation in stroke. Curr Drug Targets Inflamm Allergy 1:151–166.

Zhu C, Wang X, Qiu L, Peeters-Scholte C, Hagberg H, Blomgren K (2004) Nitrosylation precedes caspase-3 activation and translocation of apoptosis-inducing factor in neonatal rat cerebral hypoxia-ischaemia. J Neurochem 90:462–471.

Zielasek J, Hartung HP (1996) Molecular mechanisms of microglial activation. Adv Neuroimmunol 6:191–222.